Journal of Particulate Science and Technology, 26: 574-586, 2008
DOI: http://dx.doi.org/ 10.1080/02726350802498756

Artificial Neural Network Approach to Segregation Characteristic of Binary Heterogeneous Mixtures in Promoted Gas Solid Fluidized Beds

A. Sahoo and G. K. Roy*

Chemical Engineering Department, National Institute of Technology, Rourkela-769008, Orissa, India

Abstract

Binary mixtures of particles of same size but of different densities are fluidized in a 15cm diameter column with a perforated plate distributor with two co-axial promoters. In the present work an attempt has been made to study the fluidization and the segregation characteristic of solids of same size but density-variant in terms of segregation distance. The dimensionless segregation distance has been correlated with other dimensionless groups relating the various system parameters viz. ratio of the density of jetsam particles to that of flotsam, initial static bed height, height of layer of particles above the bottom grid, superficial gas velocity and average density of the mixture on the basis of dimensional analysis approach for both un-promoted and promoted beds. Correlations have also been developed with the above system parameters by using **Artificial Neural Network** approach for different types of fluidized beds and thus the findings with respect to both the approaches have been compared with each other. The segregation distance values for promoted beds have also been compared here with that of un-promoted bed in this work.

Keywords*: Segregation distance, Co-axial promoters, Heterogeneous Binary mixtures, Gas-solid fluidization and Artificial Neural Network approach.*

.....

** Corresponding author. Tel: +91-661-2463258 (R), 2462258 (O) Fax: +91-661-2472926*

E-Mail: abantisahoo@gmail.com, asahu@nitrkl.ac.in

Introduction

Segregation or de-mixing is a major problem especially encountered in gas-solid fluidization of homogeneous and heterogeneous mixtures. Segregation can even be a problem in mixers, whereby over-mixing can actually lead to segregation. More commonly, the major segregation problems occur after mixing. This may occur during discharge or transport and handling. The problem mainly occurs when there are differences in the mobility of the particles caused by different sizes, densities and/or shapes. The higher the mobility difference, the greater is the segregation. This is a prime problem with food mixes that contain bigger dried particulates mixed with powders, which may easily segregate during transport and handling after mixing. As a result, there is a need for measuring segregation tendency to give an index of the problem, a greater understanding of segregation mechanism, and procedure for trying to overcome these short-comings.

Previous studies on gas solid fluidization of multi-component solid mixture [1] have shown that particle segregation takes place, in particular, in the vertical direction of the bed when there is an appreciable density/size difference between particles. Under certain operating conditions, the segregation pattern can easily be detected by examining the vertical concentration profile of one of the components of the mixture. A bed may be fluidized in the sense that all the particles are fully supported by the gas, but may still be segregated in the sense that the local bed composition does not correspond with the overall average. Segregation is likely to occur when there is substantial difference in the drag/unit weight between different particles. Particles having a higher drag/unit weight migrate to the distributor [2].

Literature

The influence of internal baffles on the behavior of fluidized beds has been reviewed by Harrison and Grace [3] and Sitnai and Whitehead [4] for reactor designs. Z. Jun et al. [5] have observed the restriction of large scale solids movement by internal baffles thus narrowing the residence time distribution of both gas and solids in continuous beds consisting of uniform particles.

Gelperin et al. [6] were able to carryover the fines to the top of the bed using binary mixture of coal particles in a conical baffled fluidized bed. Zhang and Beeckmans [7] observed the reduction of axial mixing of particles by mechanically stirring the fluidized bed. Beeckman and Yu [8, 9] observed the continuous separation of solids to be possible using rod stirrers in a three component system using virtually bubble free fluidizing medium with the heterogeneous binary mixture. The improved separation was observed by them using the screen-like stirrers. But they observed the inferior quality separation without the fluidizing medium (a two-component system containing only particles to be separated) which was probably due to the destruction of pure jetsam layer at the bottom of the bed. Hartholt et al. [10] observed effective segregation in a batch fluidized bed using stationary horizontal-screen like baffles with a relatively large free area by varying the number of screens and the superficial velocity of the fluidizing medium.

Gibilaro and Rowe [11] have proposed a mathematical model by formulating conservation equation for jetsam particles relative to the bulk particles due to the rise of one single gas bubble in fluidized bed. Tanimoto et al. [1] have observed that the jetsam particles descent relative to the bulk particles. Thus they defined the segregation distance as the relative distance of the jetsam to the bulk particles due to the rise of one single gas bubble entrained with the particles, and measured the same by taking the difference between the two drift lines. They have also observed that more segregation takes place in the three-dimensional bed compared to a two-dimensional one.

The distance thus obtained would be equal to the mean settling distance if the region wherein drift occurred corresponded exactly with the cross-sectional area of the bubble (in fact, significant drift occurs up to a distance of three bubble radii from the center of the rising bubble). They defined the dimensionless average segregation distance (Y_s) reduced over the bubble cross sectional area. The empirical dimensionless segregation distance related to the properties of the jetsam and flotsam was proposed by Tanimoto et al. [1], as under.

$$Y_S = 0.6 \times \left(\frac{\rho_j}{\rho_b} \right) \times \left(\frac{d_j}{d_b} \right)^{0.33} \qquad (1)$$

Hoffmann and Romp [12] modified the above equation further as

$$Y_S = 0.8 \times \left(\frac{\rho_j}{\rho_b} \right) \times \left(\frac{d_j}{d_b} \right)^{0.33} - 0.8 \quad (2)$$

Dechsiri et al. [13] introduced a concentration term of the flotsam to the above equation and presented the expression for the dimensionless segregation distance as

$$Y_S = 0.8 \times \left[\frac{\rho_j \left(d_j\right)^{0.33}}{C_f \left(\rho_f \left(d_f\right)^{0.33}\right) + \left(1 - C_f\right)\left(\rho_j \left(d_j\right)^{0.33}\right)} - 1 \right] \quad (3)$$

Experimentation

The experimental set up as shown in **Fig. 1** consists of a fluidizer of 15cm ×100cm, a rotameter, a manometer, a compressor, a distributor, two promoters namely, rod and disc-type and a vacuum system. Air was used as the fluidizing medium. A binary mixture of particles of different densities but of same size with a specific mixture composition was fluidized in the fluidizer at a particular superficial gas velocity. On maintaining steady state, the samples were drawn from different heights of the bed through the side ports for analyzing the jetsam concentration at different layers under the fluidizing condition. This process was repeated by varying the different system parameters which are listed as the scope of the experiment in **Table 1(A)**. Again the whole process was repeated with two co-axial promoters namely, a rod promoter and a disc promoter, with all the other system parameters remaining constant. Details of the promoters and experimental procedure have been explained by the author reported earlier [14].

Development of Correlations

Artificial Neural Network (ANN) Approach:

An ANN-based model has been defined in literature as a computing system made up of a number of simple and highly interconnected processing elements, which processes information by its dynamic state response to external inputs. The back propagation network is the most well known and widely used among the current types of neural networks systems. The same method has been used in the present study to develop the model in the following mentioned form, where different values for the

coefficient and exponents have been determined according to the procedure described previously [14] and [15].

In the present work the network is trained with 196 data sets for each type of the fluidized bed. The network structure together with the learning rate was varied to obtain an optimum structure with a view to minimize the mean square error at the output.

$Y_S, \left(\frac{\rho_f}{\rho_j} \times \frac{\rho_m}{\rho_j}\right), \left(\frac{H_S}{D_C}\right), \left(\frac{H_b}{D_C}\right)$ and $\left(\frac{U_O}{U_{mf}}\right)$ parameters have been considered as the input parameters. K & n (overall coefficient and exponent of the correlation respectively) and a, b, c, d (individual exponents of these parameters) have been considered as the output parameters for the ANN training of the data.

The general form of the developed correlation can be represented as

$$Y_S = K\left[\left(\frac{\rho_f}{\rho_j} \times \frac{\rho_m}{\rho_j}\right)^a \left(\frac{H_S}{D_C}\right)^b \left(\frac{H_b}{D_C}\right)^c \left(\frac{U_O}{U_{mf}}\right)^d\right]^n$$

or, $$Y_S = K\left[\left(\frac{\rho_f}{\rho_j} \times \frac{\rho_m}{\rho_j}\right)^{a \times n} \left(\frac{H_S}{D_C}\right)^{b \times n} \left(\frac{H_b}{D_C}\right)^{c \times n} \left(\frac{U_O}{U_{mf}}\right)^{d \times n}\right]$$

The optimum structure of ANN training obtained from this data set for both the conditions is shown in **Fig. 2**. The error plots are shown in **Fig. 3**. In the present work the experimental segregation distance values have been calculated using **Eq. (3)** for all types of beds i.e. un-promoted and promoted (with rod and disc type promoters) fluidized beds. Correlations for the segregation distance have been developed for all types of beds using various system parameters from both the approaches viz. the dimensional analysis and the Artificial Neural Network.

The final correlations thus developed are as given below.

For un-promoted fluidized bed:

$$Y_S = 0.173 \times \left[\left(\frac{\rho_f}{\rho_j} \times \frac{\rho_m}{\rho_j}\right)^{-1.298} \left(\frac{H_S}{D_C}\right)^{0.015} \left(\frac{H_b}{D_C}\right)^{0.012} \left(\frac{U_O}{U_{mf}}\right)^{-0.003}\right] \quad (4)$$

For rod-promoted fluidized bed:

$$Y_S = 0.188 \times \left[\left(\frac{\rho_f}{\rho_j} \times \frac{\rho_m}{\rho_j}\right)^{-1.187} \left(\frac{H_S}{D_e}\right)^{0.003} \left(\frac{H_b}{D_e}\right)^{0.0014} \left(\frac{U_O}{U_{mf}}\right)^{0.0002}\right] \quad (5)$$

For disc-promoted fluidized bed:

$$Y_S = 0.1876 \times \left[\left(\frac{\rho_f}{\rho_j} \times \frac{\rho_m}{\rho_j} \right)^{-1.187} \left(\frac{H_S}{D_e} \right)^{-0.003} \left(\frac{H_b}{D_e} \right)^{0.002} \left(\frac{U_O}{U_{mf}} \right)^{-0.001} \right] \quad (6)$$

Dimensionless Analysis (DA) Approach:

Attempt has been made to correlate the segregation distance obtained from Eq. (3) with the various system parameters. The plots of the experimental segregation distance against the system parameters for all types of fluidized beds are shown in **Fig. 4, Fig. 5 and Fig. 6**. The final correlations are as follows:

For un-promoted fluidized bed:

$$Y_S = 0.186 \times \left[\left(\frac{\rho_f}{\rho_j} \times \frac{\rho_m}{\rho_j} \right)^{-1.190} \left(\frac{H_S}{D_C} \right)^{0.012} \left(\frac{H_b}{D_C} \right)^{0.011} \left(\frac{U_O}{U_{mf}} \right)^{-0.001} \right] \quad (7)$$

For rod-promoted fluidized bed:

$$Y_S = 0.188 \times \left[\left(\frac{\rho_f}{\rho_j} \times \frac{\rho_m}{\rho_j} \right)^{-1.187} \left(\frac{H_S}{D_e} \right)^{-0.003} \left(\frac{H_b}{D_e} \right)^{0.001} \left(\frac{U_O}{U_{mf}} \right)^{0.0002} \right] \quad (8)$$

For disc-promoted fluidized bed:

$$Y_S = 0.1875 \times \left[\left(\frac{\rho_f}{\rho_j} \times \frac{\rho_m}{\rho_j} \right)^{-1.186} \left(\frac{H_S}{D_e} \right)^{-0.002} \left(\frac{H_b}{D_e} \right)^{0.002} \left(\frac{U_O}{U_{mf}} \right)^{-0.0002} \right] \quad (9)$$

Results and Discussion

The mean square errors for learning of the data for the above mentioned different types of beds (sample plots up to 100 no. of epochs) are shown in **Fig. 3(a), Fig. 3(b)** and **Fig. 3(c)** respectively. For un-promoted fluidized bed, the mean square error was found to be reducing from 0.0256 at 0 (zero) number of epoch to 0.0002 at 60 numbers of epochs and this value remains constant up to 30,000 cycles (maximum number of epochs) which in turn implies the proper training of data. For rod promoted fluidized bed, the mean square error was found to be reducing from 0.018 at 0 (zero) number of epoch to 0.0 at 60 numbers of epochs and this value remains constant up to 30,000 cycles

(maximum number of epochs); where as for disc promoted fluidized bed, the mean square error was found to be reducing from 0.0142 at 0 (zero) number of epoch to 0.0 at 60 numbers of epochs and which remained constant up to 30,000 cycles (maximum number of epochs). The parameters for ANN- models for all types of beds are listed in **Table 1(B)**. The values of segregation distance were calculated by using ANN-approach and DA-approach respectively with the help of **Eq. (4)** & **Eq. (7),** for unpromoted; **Eq. (5) & (8)** and **Eq. (6) & (9)** for the rod-promoted and disc-promoted fluidized beds respectively. The calculated values from ANN-approach and DA-approach were compared with the experimental values shown in **Fig. 7, Fig. 8 and Fig.9** respectively. A good agreement has been found with the experimental values by both the methods in most of the cases for all types of fluidized beds. The mean and standard deviation for the two methods viz. for DA-approach and ANN-approach are listed in **Table 2**. Calculated values of segregation distance by ANN approach for both the types of promoted fluidized beds have been compared with those of un-promoted bed in **Fig. 10**. On comparing the calculated values of segregation distance for promoted beds with that of un-promoted bed it is found that use of promoters give lesser segregation distance than the simple fluidized bed for heterogeneous irregular binaries which probably due to the fact that the presence of promoter reduces the rising of bubbles.

It is well known that the particle drift due to the movement of bubbles causes mixing. The wakes of rising bubbles loose their wake particles due to the presence of promoters [10]. In case of rod-promoter which obstructs up to 50cm height of the column, the upward particle transport in the bed gets hindered. Wakes of rising bubbles move upward only through the gap between the promoter and the column, which limits its rise to a small distance.

For disc-promoter, five circular discs (each of 5cm.dia) have been attached to a central rod with 10cm. spacing, covering up to half the length of the column. The bubble wakes impact on these horizontal discs [16]. Thus the wakes of rising bubbles loose their wake particles and there after new wakes form above the disc/baffle. This decreases the upward particle transport in the bed [10]. Some bubbles rise through the gap between the column and promoter also thus giving some upward particle transport.

Thus both mixing and segregation processes are hindered by the promoters. But the former is the most. The result is that the bed demixes more slowly but more completely [10].

In the present work both the promoters obstruct the jetsam particle transport in upward direction along with the rising bubble thereby decreasing the segregation distance for the heterogeneous binary mixture in promoted bed than in the un-promoted bed whereas flotsam particles being lighter might have been transported upward along with the rising bubbles in a faster way during fluidization thereby demixing the bed more completely.

Although the effect of the other system parameters on the segregation distance in comparison with the density factor is not very significant, their effects on the segregation characteristic of binary mixture can not be ignored.

Conclusion

The model developed by ANN was tested against experimental values and was also compared with the model developed by dimensional analysis approach for all types of the fluidized beds. The results obtained were found to be well within the reasonable limits implying thereby its applicability to a wide range of process conditions.

The developed correlations by the ANN-approach have been completely authenticated by the DA-approach models. These developed models can widely be used for analyzing the segregation characteristics of the heterogeneous binary mixtures of particles over a good range of the operating parameters. Under identical situations, the calculated values of the segregation distance have been found to be higher for un-promoted fluidized bed than the promoted one thereby indicating improvement in segregation in promoted beds and providing a method for its potential application by using promoters both in vertical and horizontal manner in solid-solid separation based on density difference.

Nomenclature

C : Concentration of particles at any height in the bed

D_C : Diameter of the column, m

De : Equivalent diameter of the column, m

d : Particle size, m

H_b : Height of particles layer in the bed from the distributor, m

Hs : Initial static bed height, m

U : Superficial velocity of the fluidizing medium, m/s

Y_s : Segregation distance, dimensionless

ρ : Density in kg/m^3

Suffixes:

o : operating condition

mf : minimum fluidizing condition

j : jetsam

f : flotsam

b : bulk

m : mean or average for the mixture

p : particle

Abbreviations:

ANN : Artificial Neural Network

D. A. : Dimensional analysis

dens_factor : combined system variable, $\left(\frac{\rho_f}{\rho_j} \times \frac{\rho_m}{\rho_j} \right)$

ρ_{r1} : $\frac{\rho_f}{\rho_j}$

ρ_{r2} : $\frac{\rho_m}{\rho_j}$

Bibliography:

[1] Tanimoto, H.; S. Chiba, T. Chiba and H. Koboyashi, 1981, Jetsam descent induced by a single bubble passage in three-dimensional gas-fluidized beds, Journal of Chemical Engineering of Japan, , 14, 4, 273-276.

[2] Wu, S. Y. and J. Baeyens, 1998, Segregation by size difference in gas fluidized beds, Powder Technology, 98, 139-150.

[3] Harrison, D. and J. R. Grace, 1971, Fluidization, 2nd edn, in J. F. Davidson and D. Harrison (eds.), Academic Press. London,

[4] Sitnai, O. and A. B. Whitehead, 1985, Fluidization, 2nd edn in J. F. Davidson, R. Clift and D. Harrison (eds.), Academic Press. London.

[5] Jun, Z., Z. Xing and X. Heqing, 1992, A model of solid back mixing between stages in a gas-fluidized bed with perforated baffles, Powder Technology, 73, 37 – 41.

[6] Gelperin, N. I., V. G. Einstin, V. B. Kwasha, A. S. Kogan and S. A. Vil'nits, 1964, Apparatus for classification of free-flowing materials in a fluidized bed, Int. Chem. Eng., 4, 198-203.

[7] Zhang, Z. and J. M. Beeckmans, 1990, Segregation in a Stirred Fluidized Bed, Can. J. Chem. Eng., 68, 932-937.

[8] Beeckmans, J. M. and Z. Yu, 1992, Continuous Separation of Mixed Solids Using a Rotating-Screen Fluidized Bed, Can. J. Chem. Eng., 70, 1048 -1054.

[9] Beeckmans, J. M. and Z. Yu, 1992, Continuous Separation of Solids in a Mechanically Fluidized Bed, Powder Technology, 70, 77-81.

[10] Hartholt, G. P., R. la Riviere, A. C. Hoffmann and L. P. B. M. Janssen, 1997, The influence of perforated baffles on the mixing and segregation of a binary group B mixture in a gas-solid fluidized bed, Powder Technology, 93, 185-188

[11] Gibilaro, L. G. and P. N. Rowe, 1974, A Model for a Segregation Gas Fluidized Bed, Chemical Engineering Science, 29, 1403-1412.

[12] Hoffman, A.C. and E. Romp, 1991, Segregation in a Fluidized Powder of a Continuous Size Distribution. *Powder Technology* **66**, 119–126.

[13] Dechsiri, C., J. C. Bosman, H. G. Dehling, A. C. Hoffmann and G. Hui, 2001, A stochastic model for particle mixing and segregation in fluidized beds with baffles, In *Proceedings of PARTEC 2001*, Nuremberg, Germany, March-2001.

[14] Sahoo, A. and G. K. Roy, 2007, Artificial Neural Network Approach to Segregation Characteristic of Binary Homogeneous Mixtures in Promoted Gas -Solid Fluidized Beds, Powder Technology, 171, 54 -62.

[15] Sahoo, A. and G. K. Roy, 2008, Segregation Characteristics of Irregular Binaries in Gas-Solid Fluidized Beds – An ANN Approach, accepted for Journal of China Particuology, (**In press**) April-2008.

[16] Clift, R. and S. Rafailidis, 1993, Interparticle Stress, Fluid Pressure, and Bubble Motion in Gas-Fluidized Beds, Chem. Eng. Sc., 48, 1575 -1582.

Figure Caption

Fig. 1: Experimental Set-up.

Fig. 2: Optimum structure for the Artificial Neural Network.

Fig. 3: Mean square error against the maximum no. of epochs up to 100 for,

(a) Un-promoted fluidized bed

(b) Rod-promoted fluidized bed

(c) Disc-promoted fluidized bed.

Fig. 4: Experimental values of the segregation distance against system parameters used for the development of correlation by D.A.-approach for the un-promoted fluidized bed.

Fig. 5: Experimental values of the segregation distance against system parameters used for the development of correlation by D.A.-approach for the rod-promoted fluidized bed.

Fig. 6: Experimental values of the segregation distance against system parameters used for the development of correlation by D.A.-approach for the disc-promoted fluidized bed.

Fig. 7: Comparison between the calculated values of the segregation distance by both the approaches (D.A. and ANN-approach) against the experimental data for the un-promoted fluidized bed.

Fig. 8: Comparison between the calculated values of the segregation distance by both the approaches

Sl. No.	Bed Material	Density of Flotsam particles ρ_p, kg/m^3	Density of Jetsam ρ_p, kg/m^3	Ratio of jetsam to flotsam in the mixture	Average particle density of the mixture ρ_m, kg/m^3	Initial static bed height Hs, $\times 10^2$, m	Heights of layers for the withdrawal of samples, $H_b \times 10^2$, m

(D.A. and ANN-approach) against the experimental data for the rod-promoted fluidized bed.

Fig. 9: Comparison between the calculated values of the segregation distance by both the approaches (D.A. and ANN-approach) against the experimental data for the disc-promoted fluidized bed.

Fig. 10: Comparison of calculated values of the segregation distance for un-promoted and promoted fluidized beds.

Table 1(A): Scope of the experiment

1	Coal & Iron	1430	4760	25:75	2262.5	20	2,4,6,8,10,12,14,16,18,20
2	Refr.brick & Iron	2550	4760	25:75	3102.5	20	2,4,6,8,10,12,14,16,18,20
3	Latrite & Iron	3390	4760	25:75	3732.5	20	2,4,6,8,10,12,14,16,18,20
4	Dolomite & Iron	2940	4760	25:75	3395	20	2,4,6,8,10,12,14,16,18,20
5	Dolomite & Iron	2940	4760	10:90	3122	20	2,4,6,8,10,12,14,16,18,20
6	Dolomite & Iron	2940	4760	40:60	3668	20	2,4,6,8,10,12,14,16,18,20
7	Dolomite & Iron	2940	4760	50:50	3850	20	2,4,6,8,10,12,14,16,18,20
8	Dolomite & Iron	2940	4760	25:75	3395	16	2,4,6,8,10,12,14,16
9	Dolomite & Iron	2940	4760	25:75	3395	18	2,4,6,8,10,12,14,16,18
10	Dolomite & Iron	2940	4760	25:75	3395	22	2,4,6,8,10,12,14,16,18,20

Table: 1 (B)

ANN-Parameters:	Un-promoted fluidized bed	Rod-promoted fluidized bed	Disc-promoted fluidized bed
Type	Three layered, Back Error Propagation	Three layered, Back Error Propagation	Three layered, Back Error Propagation
Slope parameter (λ)	0.95	0.75	0.75
Learning _ rate (α)	0.001	0.01	0.01
Number of training	196	190	196

vectors			
Number of testing patterns	196	196	196
Maximum cycles / epochs	30000	30000	30000
Input nodes	05	05	05
No. of hidden nodes	04	04	04
No. of output nodes	06	06	06

Table 2: Deviation of the calculated values of segregation distance from the experimental ones

BED:	Un-promoted Fluidized Bed		Rod-promoted Fluidized Bed		Disc-promoted Fluidized Bed	
Approach	D.A.-approach	ANN-approach	D.A.-approach	ANN-approach	D.A.-approach	ANN-approach
Standard deviation, %	6.958	7.908	7.0141	7.0199	7.002	7.001
Mean Deviation, %	4.436	5.589	4.272	4.235	4.244	4.253

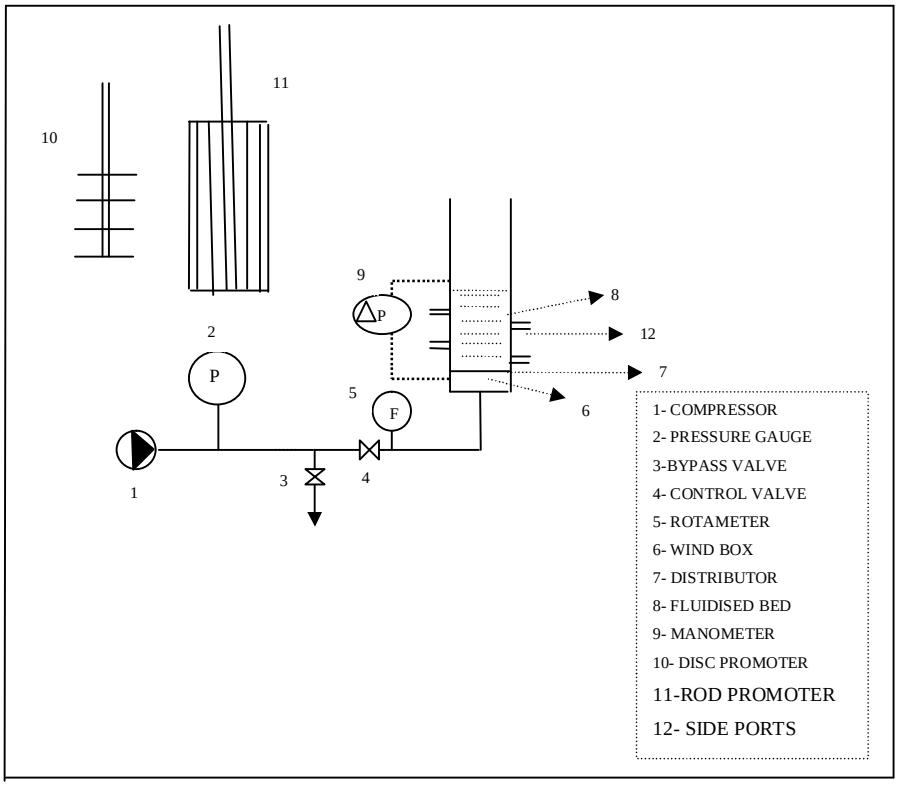
10
11
9
P
8
12
2
P
7
5
F
6
1
3
4
1- COMPRESSOR
2- PRESSURE GAUGE
3-BYPASS VALVE
4- CONTROL VALVE
5- ROTAMETER
6- WIND BOX
7- DISTRIBUTOR
8- FLUIDISED BED
9- MANOMETER
10- DISC PROMOTER
11-ROD PROMOTER
12- SIDE PORTS

Fig. 1

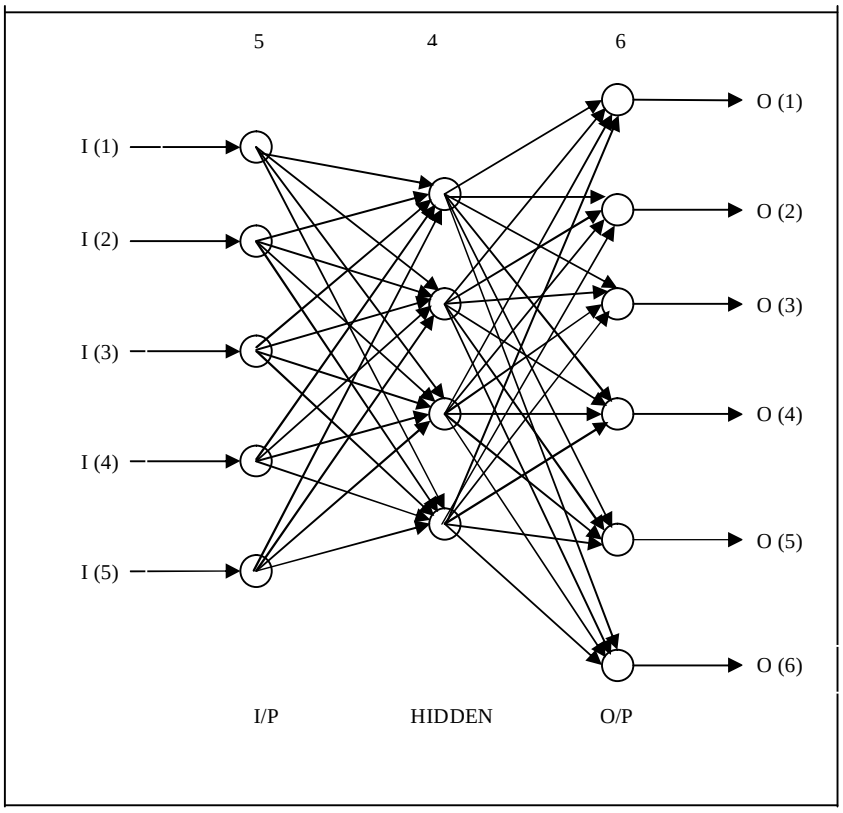
5
4
6
I (1)
I (2)
I (3)
I (4)
I (5)
O (1)
O (2)
O (3)
O (4)
O (5)
O (6)
I/P
HIDDEN
O/P

Fig. 2

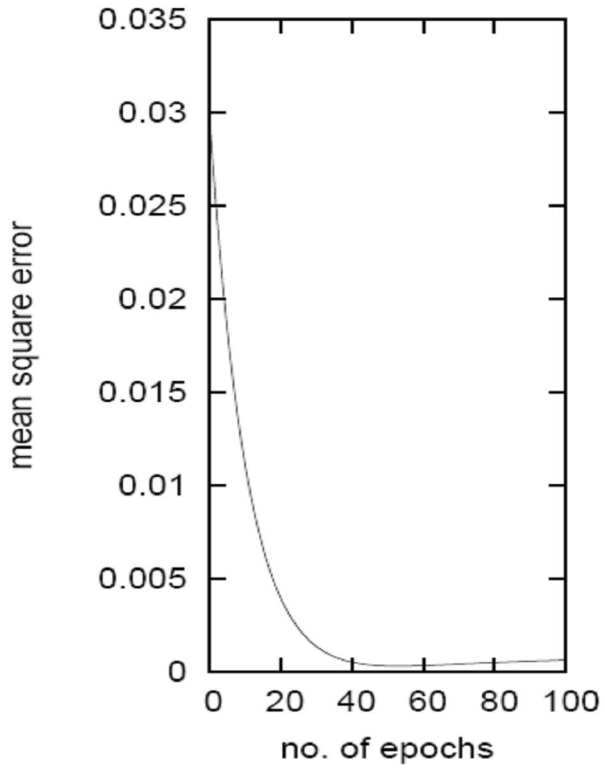
0.035
0.03
0.025
0.02
0.015
0.01
0.005
0
mean square error
0
20
40
60
80
100
no. of epochs

Fig.3 (a)

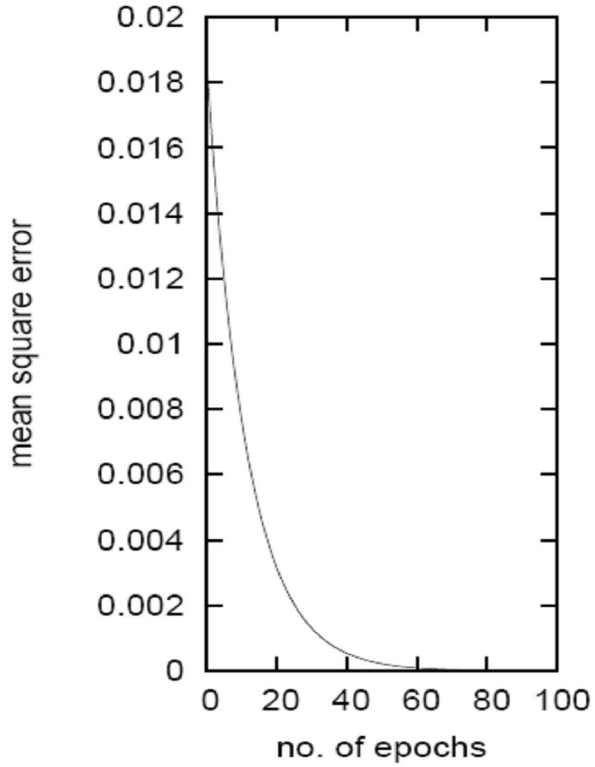
0.02
0.018
0.016
0.014
0.012
0.01
0.008
0.006
0.004
0.002
0
mean square error
0
20
40
60
80
100
no. of epochs

Fig. 3 (b)

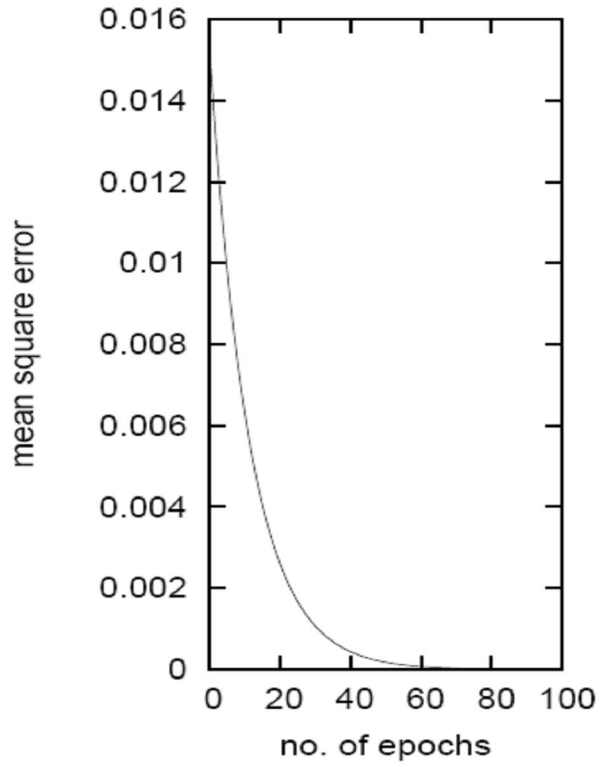
0.016
0.014
0.012
0.01
0.008
0.006
0.004
0.002
0
mean square error
0 20 40 60 80 100
no. of epochs

Fig. 3 (c)

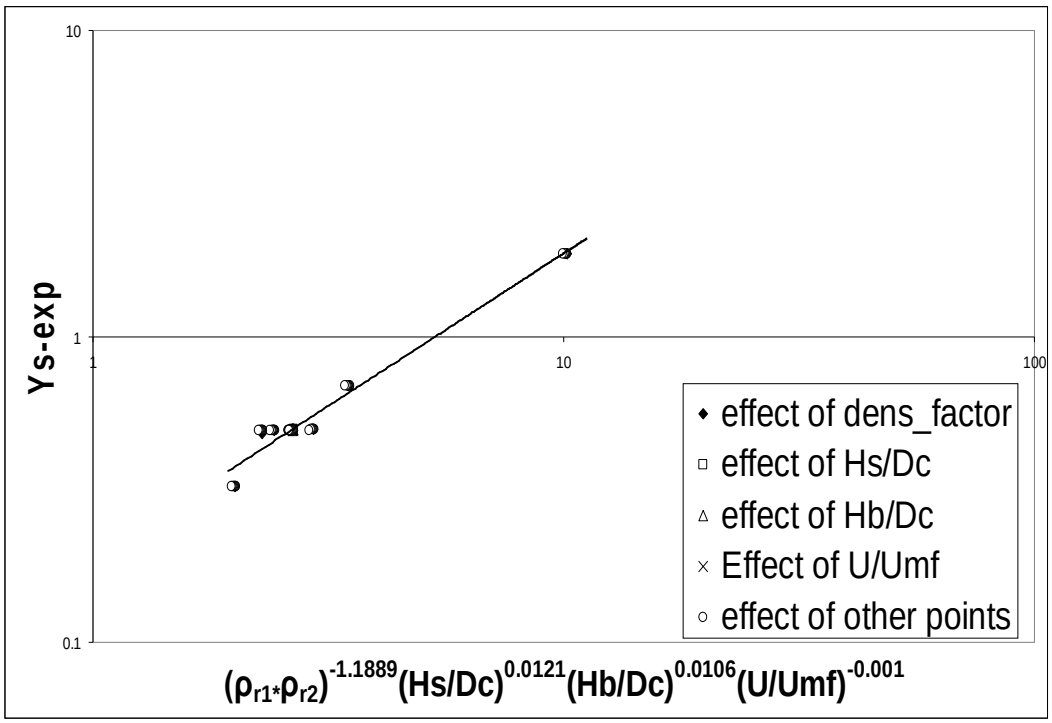
10
1
0.1
1
10
100
Ys-exp
effect of dens_factor
effect of Hs/Dc
effect of Hb/Dc
Effect of U/Umf
effect of other points
(ρr1*ρr2)-1.1889(Hs/Dc)0.0121(Hb/Dc)0.0106(U/Umf)-0.001

Fig. 4

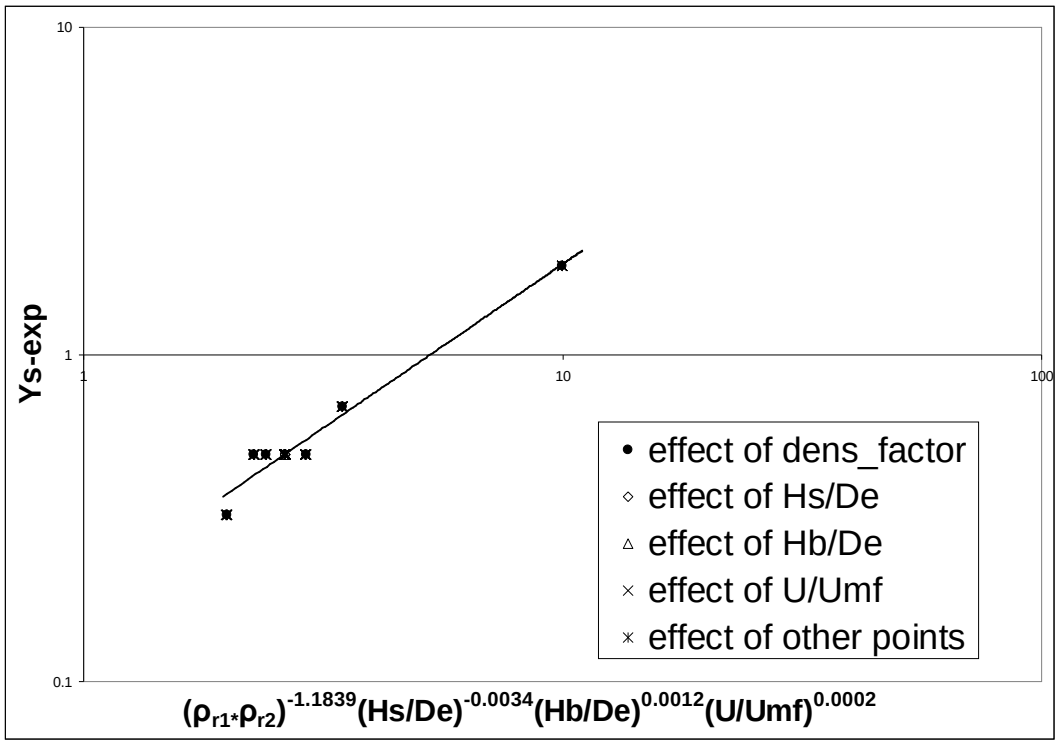
10
1
0.1
1
10
100
Ys-exp
effect of dens_factor
effect of Hs/De
effect of Hb/De
effect of U/Umf
effect of other points
$(\rho_{r1}*\rho_{r2})^{-1.1839}(Hs/De)^{-0.0034}(Hb/De)^{0.0012}(U/Umf)^{0.0002}$

Fig. 5

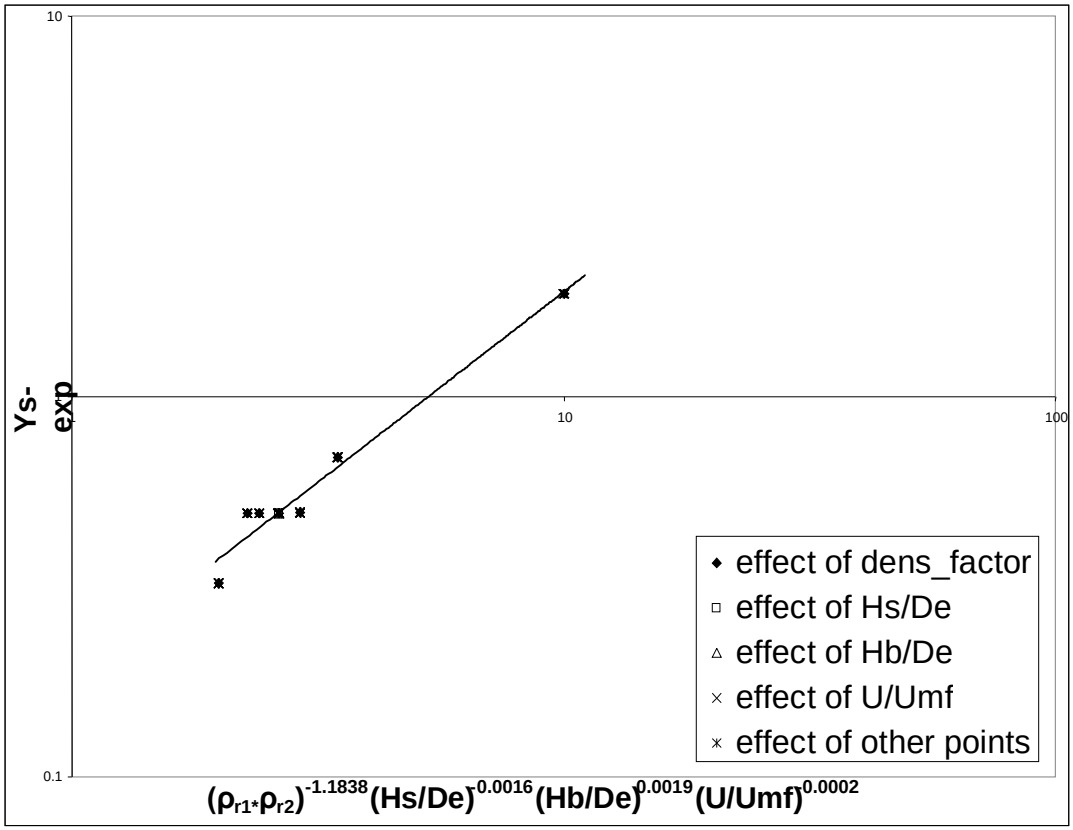
10
0.1
1
10
100
Ys-exp
effect of dens_factor
effect of Hs/De
effect of Hb/De
effect of U/Umf
effect of other points
$(\rho_{r1}*\rho_{r2})^{-1.1838}(Hs/De)^{-0.0016}(Hb/De)^{-0.0019}(U/Umf)^{0.0002}$

Fig. 6

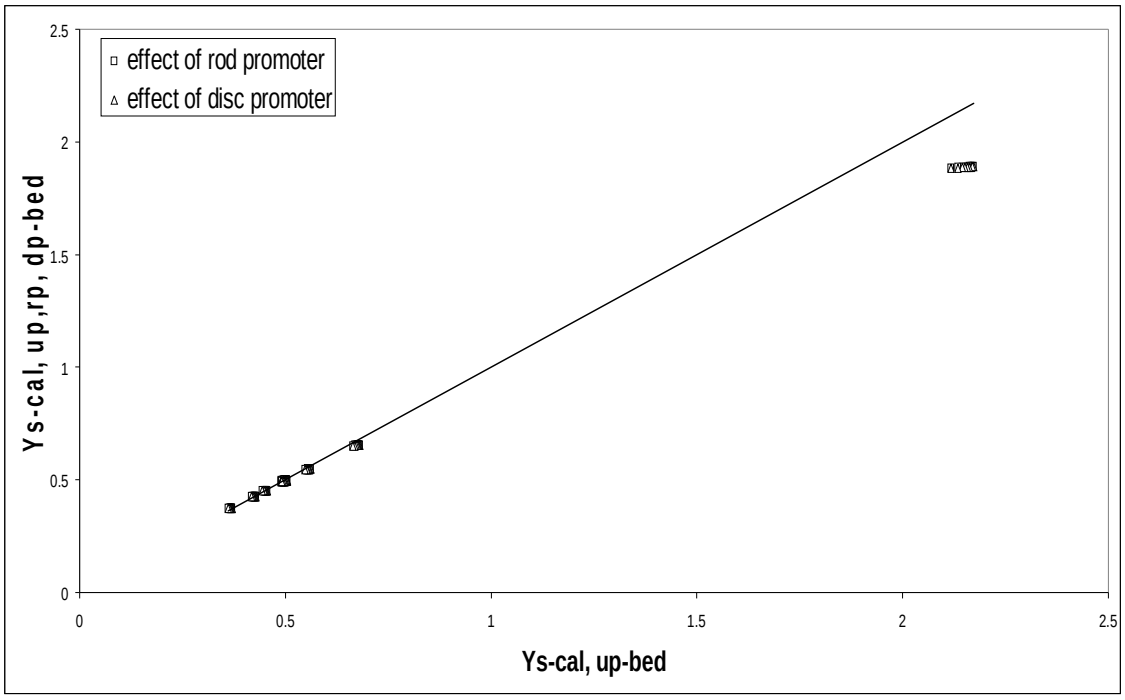
effect of rod promoter
effect of disc promoter
Ys-cal, up,rp, dp-bed
Ys-cal, up-bed
0
0.5
1
1.5
2
2.5

Fig. 7

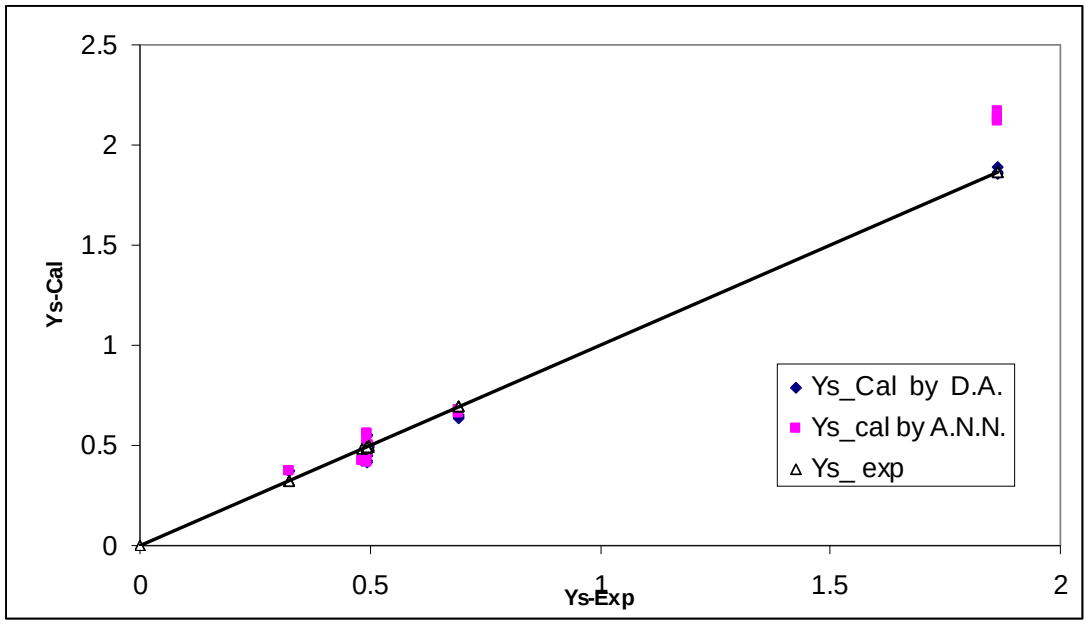
Ys_Cal by D.A.
Ys_cal by A.N.N.
Ys_ exp
Ys-Cal
Ys-Exp
0
0.5
1
1.5
2
2.5

Fig. 8

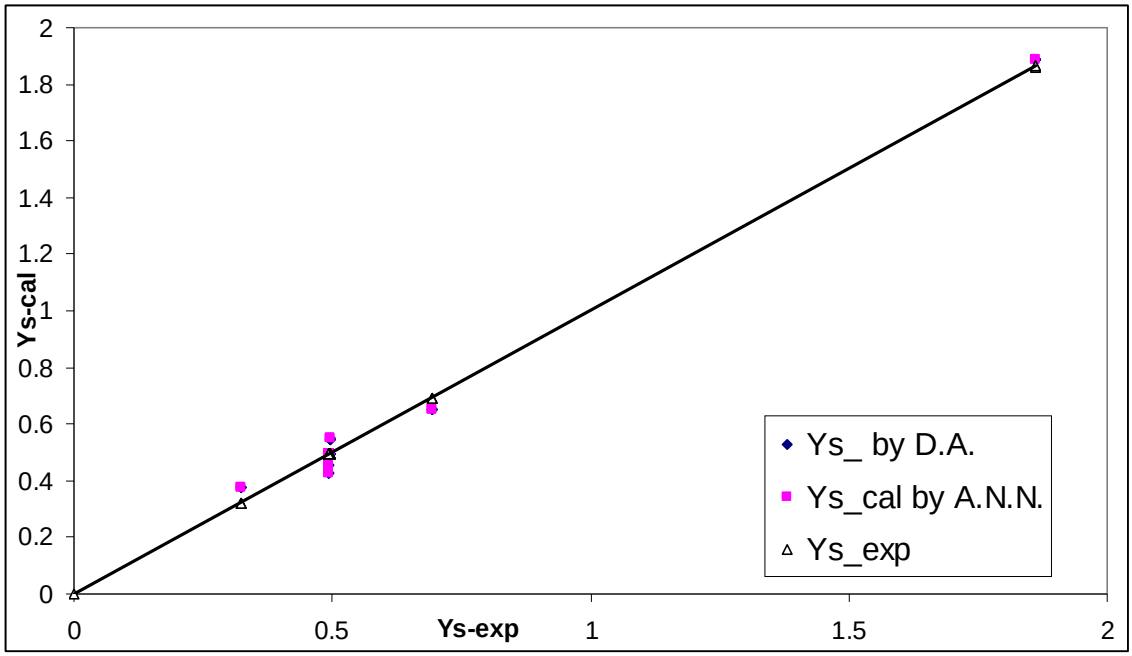
Ys-cal
Ys-exp
Ys_ by D.A.
Ys_cal by A.N.N.
Ys_exp

Fig. 9

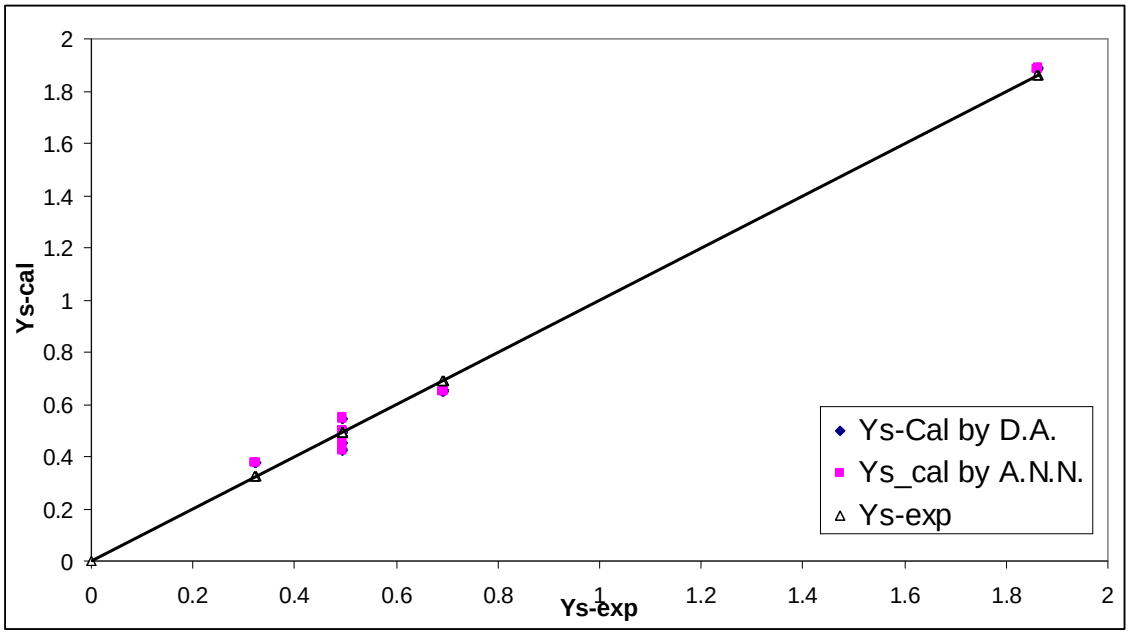
Ys-cal
Ys-exp
Ys-Cal by D.A.
Ys_cal by A.N.N.
Ys-exp

Fig. 10